Available online at www.sciencedirect.com
SCIENCE DIRECT®
Biomaterials 26 (2005) 7587–7595
Biomaterials
www.elsevier.com/locate/biomaterials

Nano-C_{60} cytotoxicity is due to lipid peroxidation

Christie M. Sayes[a], Andre M. Gobin[b], Kevin D. Ausman[c], Joe Mendez[a], Jennifer L. West[b,c,*], Vicki L. Colvin[a,c]

[a]*Department of Chemistry, 6100 Main St. MS-60, Rice University, Houston, TX 77005, USA*
[b]*Department of Bioengineering, 6100 Main St. MS-142, Rice University, Houston, TX 77005, USA*
[c]*Center for Biological and Environmental Nanotechnology, 6100 Main St. MS-63, Rice University, Houston, TX 77005, USA*

Received 8 April 2005; accepted 16 May 2005
Available online 11 July 2005

Abstract

This study examines the biological effects of water-soluble fullerene aggregates in an effort to evaluate the fundamental mechanisms that contribute to the cytotoxicity of a classic engineered nanomaterial. For this work we used a water-soluble fullerene species, nano-C_{60}, a fullerene aggregate that readily forms when pristine C_{60} is added to water. Nano-C_{60} was cytotoxic to human dermal fibroblasts, human liver carcinoma cells (HepG2), and neuronal human astrocytes at doses $\geqslant 50$ ppb ($LC_{50} = 2$–50 ppb, depending on cell type) after 48 h exposure. This water-soluble nano-C_{60} colloidal suspension disrupts normal cellular function through lipid peroxidation; reactive oxygen species are responsible for the membrane damage. Cellular viability was determined through live/dead staining and LDH release. DNA concentration and mitochondrial activity were not affected by the nano-C_{60} inoculations to cells in culture. The integrity of cellular membrane was examined by monitoring the peroxy-radicals on the lipid bilayer. Subsequently, glutathione production was measured to assess the cell's reaction to membrane oxidation. The damage to cell membranes was observed both with chemical assays, and confirmed physically by visualizing membrane permeability with high molecular weight dyes. With the addition of an antioxidant, L-ascorbic acid, the oxidative damage and resultant toxicity of nano-C_{60} was completely prevented.

Keywords: Nanoparticle; Cytotoxicity; Nano-C_{60}; Membrane oxidation

1. Introduction

Water-soluble fullerene systems are promising candidates for many medical technologies and have been proposed as crucial components for emerging electronic, optical and mechanical materials [1,2]. Given the widespread applications and their impending commercialization, both humans and environmental systems will be increasingly exposed to materials like C_{60} in the near future; thus, early evaluations of their health effects are valuable [3]. Previously, we have evaluated the differential cytotoxicity of a series of water-soluble fullerene species and concluded that changes in the fullerene cage structure had substantial impact on in vitro cytotoxicity [4]. As the number of hydroxyl or carboxyl groups on the surface of the fullerene cage was increased, cytotoxicity decreased over seven orders of magnitude. The series of water-soluble fullerenes included nano-C_{60}, tris-malonic acid-C_{60} (or C_3), $Na^{+}_{2-3}[C_{60}O_{7-9}(OH)_{12-15}]^{(2-3)-}$, and $C_{60}(OH)_{24}$. Using two separate methods, we determined that the nano-C_{60} generated substantially more reactive oxygen species (ROS) than the other species under cell-free conditions. The ROS generation monotonically decreased with increasing derivatization of the fullerene cage. The dramatic cytotoxicity observed for nano-C_{60} warranted further evaluation as presented here. Additional studies were also conducted to probe the mechanisms governing the

*Corresponding author. 6100 Main Street, MS-142, Rice University, Houston, TX 77005, USA. Tel.: +1 713 348 5955.
E-mail address: jwest@rice.edu (J.L. West).

0142-9612/$ - see front matter © 2005 Elsevier Ltd. All rights reserved.
doi:10.1016/j.biomaterials.2005.05.027

cytotoxicity of nano-C_{60} and confirm the importance of oxidation.

Water-soluble fullerene derivatives are most commonly formed by deliberate synthetic methodologies and typically have altered cage chemistry and high (>100 ppm) water solubility. In contrast, the nano-C_{60} colloid investigated here is only sparingly soluble; it is produced by the addition of organic soluble C_{60} to water [5–8]. The same substance is also found when solid C_{60} is stirred in tap water for 2 months [9]. Because of its ease of formation, and stability in water, nano-C_{60} is likely to be an important form of C_{60} in natural aqueous systems.

The full characterization of the nano-C_{60} water suspension is published in two separate reports [4,10]. Proof of the presence of C_{60} in the aqueous suspension include electron diffraction via cryo-TEM, chromatographic profiles and signature spectroscopic peaks identify the presence of C_{60} in the aqueous solution. In addition, microscopy images show the size, shape and crystallinity of the C_{60} colloids. While the method of nano-C_{60} preparation may leave intercalated THF, mass spectroscopy and liquid chromatography prove that more than 90% by weight of the suspension is C_{60}, i.e. $<10\%$ of the suspension is residual solvent. Viability controls confirm that this residual solvent does not contribute to cell death or generation of ROS. The structural of the nano-C_{60} colloid consists of a pristine C_{60} core (of 10–1000 C_{60} molecules, depending on size of crystal) surrounded by a low derivatized C_{60} layer that forces the aggregate to be miscible in the aqueous phase. The extent of the derivatization is 3 groups or less, composed of either hydroxylated or oxidized fullerenes (confirmed by nuclear magnetic resonance and Fourier transform infrared spectroscopy). The negative surface charge of the aggregate is further evidence of a hydrophilic surface derivation. Because of this low degree of derivatization, we cannot fully identify the exact chemical composition of these groups.

Previous reports by Oberdorster suggest the brain and liver of largemouth bass produce changes in glutathione production once exposed to nano-C_{60}. Therefore, we hypothesize that the human cell lines hDF, Human liver carcinoma cells (HepG2), and NHA might be affected by nano-C_{60}. More specifically, within these cell lines, we concentrated on examining the effect of nano-C_{60} on the membrane of the cell, since we previously reported that nano-C_{60} produces oxygen radicals in water.

2. Materials and methods

All chemicals were purchased through Sigma Aldrich at highest purity unless otherwise stated and experiments were performed minimally in triplicate. Data are presented as mean $\pm$ standard deviation, and a student's t-test was used to determine significance.

2.1. Nano-C_{60} preparation

C_{60} was suspended in water using the method of Deguchi et al. [7] C_{60} (99.5%, MER Corporation), was dissolved in tetrahydrofuran (THF, Fisher Scientific) at a concentration of 100 mg/L. The solution was sparged with nitrogen and stirred overnight in the dark. The solution was then filtered through a 0.22 μm nylon filter (Osmonics, Fisher Scientific). MilliQ water was added to an equal volume of C_{60} in THF at a rate of 1 L/min. This solution was evaporated to eliminate the THF using a rotary evaporator (Buchii). Mass spectroscopy of solvent after this procedure finds no residual THF in solution. A 1 L mixture was evaporated to 450 mL, refilled to 550 mL with MilliQ water, and then again evaporated to 450 mL. The volume was adjusted to 550 mL again, and then evaporated to 500 mL. This final solution was stored overnight and then filtered through a 0.22 μm nylon filter to yield a suspension of aggregated C_{60} in water referred to as nano-C_{60}. $C_{60}(OH)_{24}$ was obtained from MER Corporation at 99.8% purity.

2.2. Cytotoxicity/viability

Human dermal fibroblasts (HDF) (Cambrex) were cultured in Dulbecco's Modification of Eagles Media (DMEM) with 10% fetal bovine serum and 2 mM L-glutamine, 100 U/mL penicillin, and 1 μg/mL and streptomycin. HepG2 (American Type Culture Collection) were cultured in minimal essential media (MEM) with 10% fetal bovine serum and 2 mM L-glutamine, 100 U/mL penicillin, and 1 μg/mL and streptomycin. Neuronal human astrocytes (NHA) (Cambrex) were cultured in Astrocyte Basal Medium (ABM^{TM}) derived from MCBB131 classical media with 10% fetal bovine serum and 1.5% rhEGF, 2.5% insulin, 1% ascorbic acid, 1% gentamicin sulfate and amphotericin-B, and 10% L-glutamine. For all three cell types, passage numbers 2–10 were used in the experiments. 5 μL calcein AM and 20 μL ethidium homodimer (Molecular Probes) in 10 mL phosphate buffer solution were used to determine cell viability following 48 h exposure to fullerenes. Fullerenes (nano-C_{60}) suspended in ultrapure water and sterilized via filtration (0.22 μm) were added to cells, grown in 24 well plates, at concentration of 0.24, 2.4, 24, 240 and 2400 ppb. For each experiment, the viability of untreated HDF, HepG2, and NHA cells, as well as cells treated with phosphate buffered saline (PBS) solution, was evaluated as well. Cell viability was evaluated via fluorescence microscopy (Zeiss Axiovert 135). The experiment was repeated six times.

2.3. Lactate dehydrogenase release

The release of lactate dehydrogenase (LDH) was also monitored over the nano-C_{60} concentration range described above. Cells (HDF, HepG2, NHA) were seeded in 24-well plates, exposed to nano-C_{60}, and incubated for 48 h. After incubation, the cell media was transferred to 15 mL centrifugation tubes (total volume 4 mL) and were centrifuged at 300g for 4 min. The media was decanted and analyzed for LDH release as previously described [11,12]. Upon addition of assay solutions, the media was protected from the light for 30 min. During this inoculation time, NAD is reduced to NADH using the LDH released in the medium. 400 μL of 1 N HCl was then

added to each sample to terminate the reduction of NADH. The resulting absorbance was measured at 490 nm.

2.4. Mitochondrial activity

The 1-(4,5-dimethylthiazol-2-yl)-3,5-diphenylformazan (MTT) assay (Sigma) was used to evaluate mitochondrial activity [13]. Cells, grown in 24-well plates, were exposed to fullerenes as described above. After 48 h, 150 μL of MTT (5 mg/mL) was added to each well and incubated for 4 h. Afterwards, 850 μL of the MTT solubilization solution (10% Triton X-100 in 0.1 N HCl in anhydrous isopropanol) was added to each well. The 24-well plate was gently mixed on a gyratory shaker to solubilize the formazan crystals. After solubilization in acidic isopropanol, the product was quantified by measuring absorbance at 570 nm.

2.5. DNA content

Using the fluorescent DNA-binding dye PicoGreen® (Molecular Probes), the concentration of DNA in normal HDF, HepG2, and NHA cells and cells dosed with 240 ppb nano-C_{60} was measured. A TE buffer solution (10 mM Tris-HCl, 1 mM EDTA, pH 7.5) was used to prepare the PicoGreen® dsDNA quantitation solution. An equal volume of the PicoGreen® quantitation solution was added to each HDF, HepG2, and NHA lysed sample solution. After 5 min of incubation, absorbance was measured using a spectrofluorometer (excitation 480 nm, emission 520 nm). A standard curve (1 ng/mL–1 μg/mL) was made using a DNA stock solution. Total protein was measured in cellular homogenates using the Bradford method [14,15], and DNA content was normalized to protein content.

2.6. Permeability of the plasma membrane

The integrity of the plasma membrane was examined by monitoring the uptake of fluorescein-derivatized dextrans (Molecular Probes) of increasing molecular weights (10,000–500,000 Da). Cells were treated with fullerenes as described above. After cells were washed with phosphate-buffered saline (PBS, pH 7.4), 2.5 mg/mL dextran was added to each well and then incubated at 37 °C/5% CO_2 for 30 min. Cells were washed with PBS then fixed with 5% glutaraldehyde (Sigma) and observed via fluorescent and phase contrast microscopy (Zeiss Axiovert 135).

2.7. Lipid peroxidation

Lipid peroxidation was measured in HDF, HepG2, and NHA cells using the thiobarbituric acid (TBA) assay for malondialdehyde [16] and normalized to total protein. Cells were homogenized in 50 mM HEPES-buffered saline (pH 7.2) with 0.1 mM phenylmethanesulfonyl fluoride (PMSF) using a glass tissue tearor. The homogenate was centrifuged at 14,000*g* for 5 min. 1.4 mL of 0.02% butylated hydroxytoluene (BHT) and 0.375% TBA were incubated with 100 μL of each homogenate for 15 min at 100 °C. The samples were cooled, centrifuged (5900*g* for 5 min), and the appearance of malondialdehyde was measured in the supernatant at 532 nm and compared to a standard curve containing 0–3.2 μM malondialdehyde. Total protein was measured in tissue homogenates using the Bradford method [14,15] and lipid peroxidation was normalized to protein content.

To confirm the evidence of lipid peroxidation, HDF, HepG2, and NHA cells were dosed with the nano-C_{60} solution as described above; and C11-BODIPY$^{581/591}$ (Molecular Probes) was used to monitor lipid peroxidation in cultured cells [17]. This lipophilic fluorophore changes its fluorescence when it interacts with peroxyradicals. The oxidation of C11-BODIPY$^{581/591}$ was evaluated via fluorescence microscopy (Zeiss Axiovert 135). The degree of peroxidized lipids was quantified by spectrometrically measuring the loss of red fluorescence and gain of green fluorescence (Molecular Devices SpectraMax Plus^{384}).

2.8. Glutathione production

Glutathione production was monitored for HDF, HepG2, and NHA cells exposed to nano-C_{60} at varying concentrations (0.24–2400 ppb). Control cells were treated with an equivalent volume of MilliQ water. After 48 h, cells were homogenized in 5% sulfosalicylic acid (SSA) via glass tissue tearor. The homogenate was centrifuged at 14,000*g* for 5 min. After 10 min incubation at 37 °C, 15 μL of 50 U/mL glutathione reductase was added to each sample. Absorbance at 412 nm was then measured. Glutathione standards (0–4 μM) with 100 μL NADPH, 15 μL 5,5′-dithiobis(2-nitrobenzoic acid) (DTNB), and 25 μL SSA were evaluated similarly for comparison. Total protein was measured in tissue homogenates using the Bradford method [14,15] and total glutathione was normalized to protein content.

2.9. Addition of ascorbic acid

A 1 mM L-ascorbic acid solution was prepared. HDFs were incubated in appropriate media and inoculated with 60 μL of 50 mg/L nano-C_{60}, as described above. After 40 h, 240 μL of 1 mM L-ascorbic acid was added to the HDFs. 8 h later, the lipid peroxidation assay was performed as described above.

3. Results

Cell viability was determined following 48 h exposure to fullerenes. We previously found that LDH release does not occur at 1, 12, or 30 h after inoculation with the nano-C_{60}. For this reason, all LDH measurements were performed after 48 h. The LC_{50} values, determined from the dose response curves shown in Fig. 1, are as follows: for the HDF cells, 20 ppb; for HepG2, 50 ppb; and for NHA cells, 2 ppb. Since substantial cytotoxicity was observed for nano-C_{60}, the mechanisms by which nano-C_{60} damages cells in culture were examined. Using the MTT assay, we found that mitochondrial activity was unchanged. Using the PicoGreen® DNA assay, we determined that there was no difference in DNA

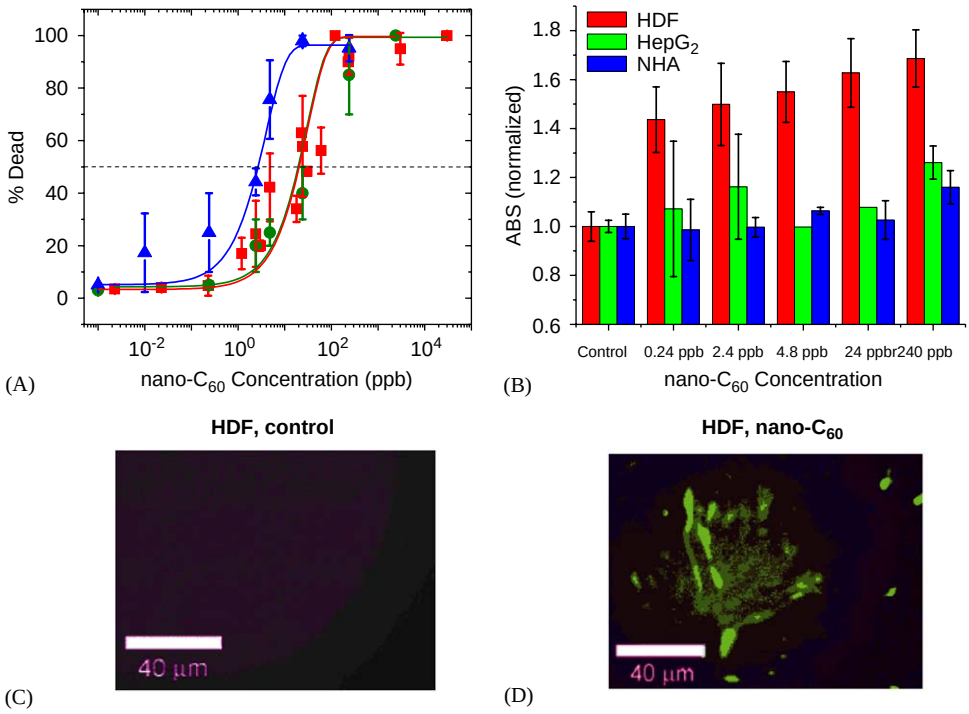

Fig. 1. The response of aggregated water-soluble fullerene species on HDF, HepG2, and NHA are dependant on nanoparticle dose and surface chemistry. All assays were performed in culture. (A) The dose response curve of the nano-C_{60} species on (■) HDF, (●) HepG2, and (▲) NHA cells. A non-linear curve fit was applied to three separate data sets. For some data points, the symbol is too large for errors bars to be seen. (B) Death of HDF, HepG2, and NHA cells via nano-C_{60} was confirmed with the lactate dehydrogenase release. Dextran fluorescein (500,000 kDa) was added to (C) normal healthy cells and (D) cells dosed with 10 ppm nano-C_{60}. Part C shows data for HDF cells only.

concentration on a per cell basis between controls or cells exposed to 2400 ppb nano-C_{60} (Fig. 2).

In the presence of nano-C_{60}, there appears to be significant membrane disruption. The membrane permeability was evaluated for HDF, HepG2, and NHA cells using fluorescent dextrans. Results for all three cell lines show that cells grown under normal conditions, without the addition of the fullerene species, uptake of fluorescent dextran was only observed with the smallest (10 kDa) dye. However, the cells dosed with 240 ppb nano-C_{60} were permeable to the 10, 70, and 500 kDa dyes (Fig. 1).

Membrane oxidation was qualitatively examined using two separate methodologies. In the first method, lipid peroxidation was indirectly measured by monitoring the production of MDTA from the oxidation of malondialdehyde in the presence of cells in culture. A gradual increase of MDTA, which corresponds to an increase of peroxyradicals on membranes, was observed for cells dosed with 0.24–4.8 ppb; and a dramatic increase of MDTA was observed for cells dosed with 240 and 2400 ppb (Fig. 3a). Additionally, the concentration of glutathione, a natural-occurring antioxidant, noticeably increases at the 240 ppb nano-C_{60} concentration (Fig. 3b) in HDF, HepG2, and NHA cells. We believe this demonstrates an increase in glutathione synthesis by the cells in response to oxidative stress. The cells could be exporting oxidized glutathione to the media, as well as synthesizing intracellular reduced glutathione.

Further evidence of lipid peroxidation is shown in Fig. 4. The second method of detecting lipid peroxidation utilizes the lipophilic fluorescent dye C11-BODIPY$^{581/591}$. This fluorescence assay was developed for localization and quantification of lipid oxidation in living cells [17]. The oxidative sensitivity of C11-BODIPY$^{581/591}$ provides indication that conditions favoring oxidation of the dye exist at the surface of the membrane. Once oxidized, the fluorescence of this dye shifts from red to green. The probe incorporates readily into cellular membranes and is about twice as sensitive to oxidation compared to probes such as cis-parinaric acid [18]. Using confocal microscopy, the oxidation of C11-BODIPY$^{581/591}$ can be visualized at the cellular level. Over time, in the presence of normal cellular membranes, the C11-BODIPY$^{581/591}$ fluorophore maintained red fluorescence (610 nm) with no green fluorescence (510 nm). However, in the presence of nano-C_{60}, the BODIPY fluorophore decreased in red fluorescence and increased in green fluorescence, indicating membrane oxidation.

In an additional set of studies, L-ascorbic acid was added to the cells during exposure to nano-C_{60} as a test to determine if the oxidative damage to HDFs could be

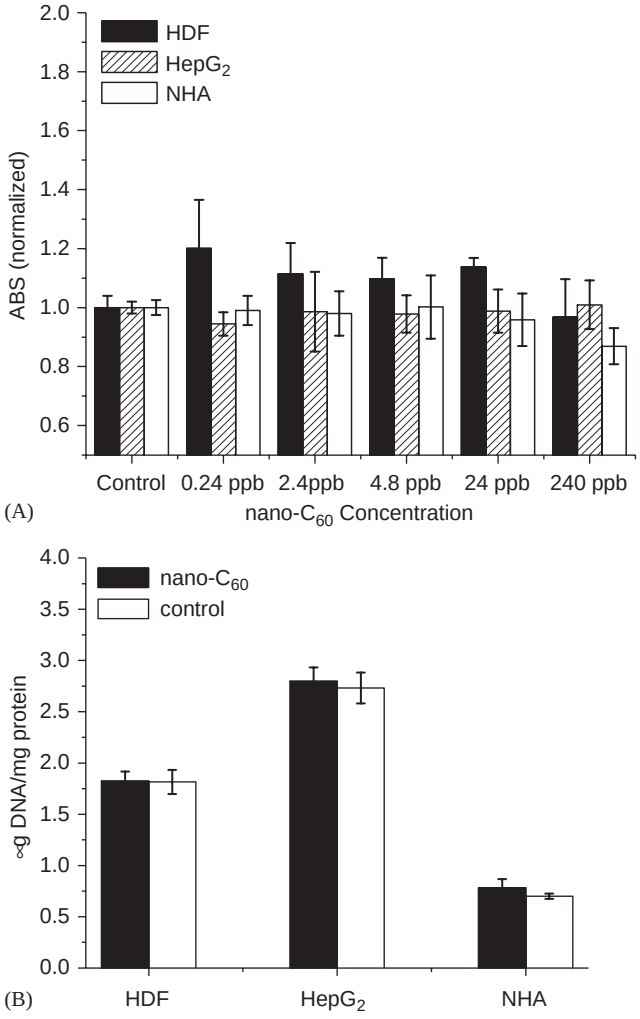

Fig. 2. Nano-C_{60} does not disrupt the mitochondrial activity or DNA concentration of HDF, HepG2, and NHA. (A) The concentration of mitochondrial dehydrogenase does not increase as nano-C_{60} concentration increases. (B) Also, the concentration of DNA in HDF, HepG2, and NHA cells before dosing is equivalent to DNA in cells after dosing and fits within the standard curve. All cells were seeded at 70% confluency. Cells were exposed to nano-C_{60} for 48 h.

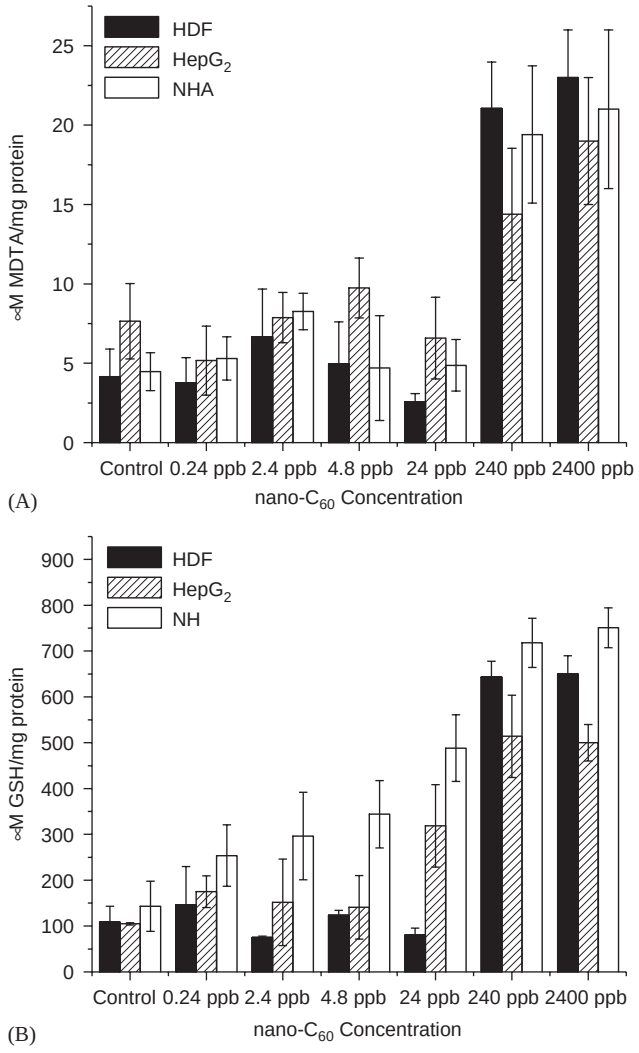

Fig. 3. The proposed mechanism in which nano-C_{60} disrupts normal cellular function. The oxy-radical produced from the solvent extraction of C_{60} from the organic solvent to water attacks the lipid bilayer of the cytoplasmic membrane, producing a peroxyradical resulting in holes in the bilayer. There is no indication of protein oxidation in any cell lines. (A) However, HDF, HepG2, and NHA cells exhibit a hysteretic lipid peroxidation curve in the form of eventual increase in μM MDTA concentration. (B) However, with the addition of ascorbic acid to the system, lipid peroxidation is prevented. In addition, the glutathione production also dramatically increases at the 240 ppb mark for the dermal and liver carcinoma, and astrocyte cell lines.

prevented (Fig. 5). After 48 h, the cells were monitored for viability and lipid peroxidation. Results show that no oxidative damage occurred when both nano-C_{60} and L-ascorbic acid was added to HDF cells. Further, cell viability was unchanged from controls when cells were treated with both nano-C_{60} and L-ascorbic acid.

4. Discussion

We investigated the effect of water-soluble fullerene aggregates, nano-C_{60}, on HDF, HepG2, and NHA cells in culture. Nano-C_{60} demonstrated significant toxicity in previous cell culture studies, while a highly hydroxylated, water-soluble fullerene, $C_{60}(OH)_{24}$ did not [4]. In these studies, we have determined that lipid peroxidation and resultant membrane damage are responsible for the cytotoxicity of nano-C_{60}. In addition, the oxidative damage and toxicity of nano-C_{60} were prevented by addition of L-ascorbic acid to the culture medium as an antioxidant.

Our findings on derivatized fullerenes agree with previous studies already established in the literature, but add additional insight into the mechanisms that dictate the differential cytotoxicity of various water-soluble fullerene species. This is the first study that investigates the interaction of nano-C_{60} with human cells in culture. Further, the few cell culture experiments involving other

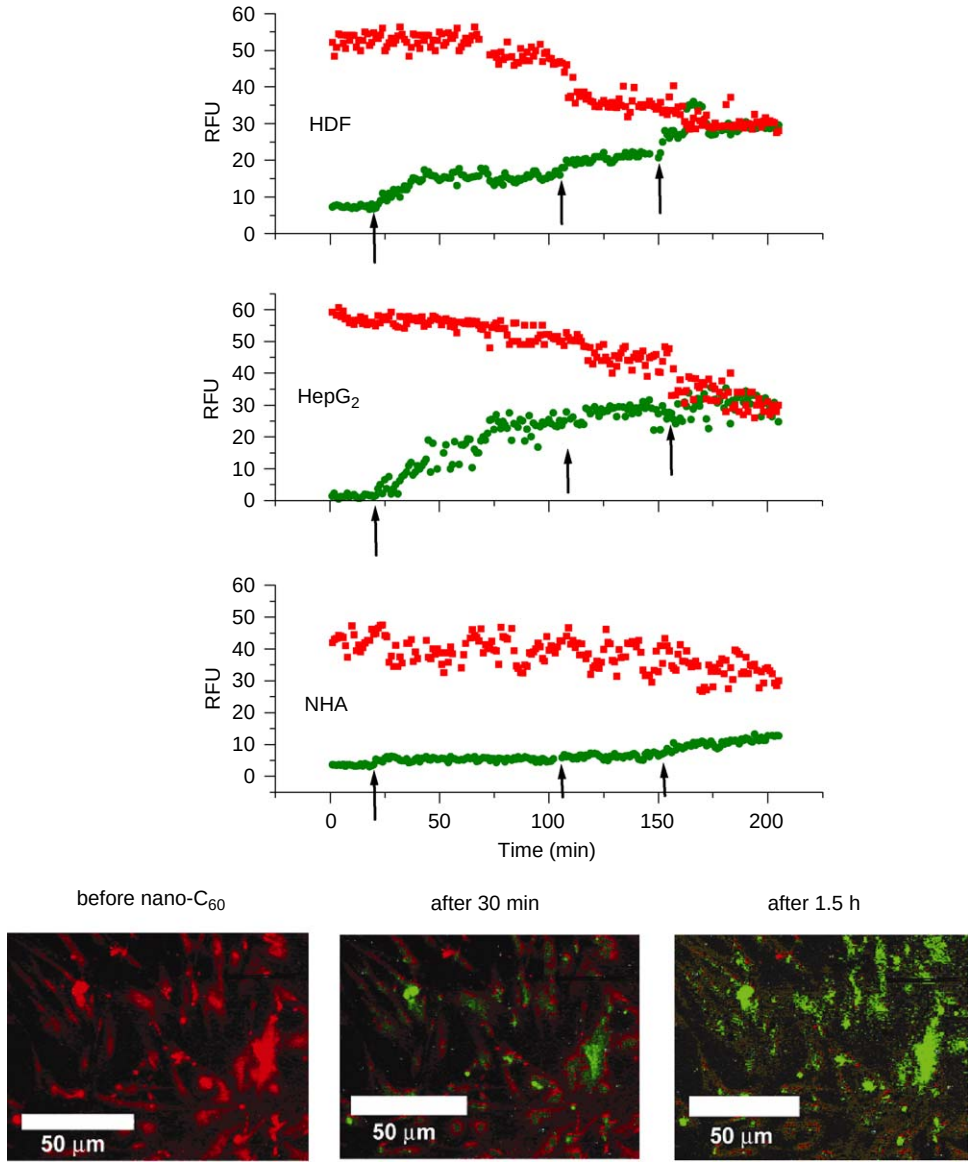

Fig. 4. The peroxidation of the lipid bilayer of cells inoculated with nano-C_{60}: HDF (top), HepG2 (middle), and NHA (bottom). The oxidation of C11-BODIPY$^{581/591}$ fluorophore is monitored simultaneously at 510 nm and 610 nm. Red fluorescence (■) 581/610 nm; green fluorescence (●) 484/510 nm. Arrows indicate points of nano-C_{60} inoculation.

types of nanoparticles, metal oxides and quantum dots, have identified particles within or around the mitochondria [4,19–21]. We have found that the water-soluble fullerene nanoparticles used in this study do not affect mitochondrial activity, but have not specifically evaluated intracellular localization of the nano-C_{60}.

Our observation of membrane oxidation is not unexpected given that ROS have been observed in aqueous solutions of water-soluble fullerenes [22]. However, our cytotoxicity is several orders of magnitude higher than that seen for other forms of fullerenes including C_3, $C_{60}(OH)_{12}$, and $C_{60}(OH)_{18-25}O_{3-7}$ [23–25]. We believe that the difference can be accounted for by the substantial fraction of pristine C_{60} in the interior of the nanocrystalline aggregates. In its underivatized form, C_{60} has a very high reduction potential and would be a good electron acceptor in biological media.

These data unambiguously show that membrane oxidation occurs in a wide variety of cell lines when exposed to nano-C_{60}. Given our prior data in cell free systems [4], which show these species capable of generating superoxide anions, we speculate that nano-C_{60} itself is the origin of the oxygen radicals, and hence a prooxidant. This behavior is distinctive from the antioxidant behavior found for other types of water-soluble fullerenes [26–33]. We can reconcile these two observations by first realizing that the chemical structure of nano-C_{60} is different from intentionally water solubilized materials. This should lead to different

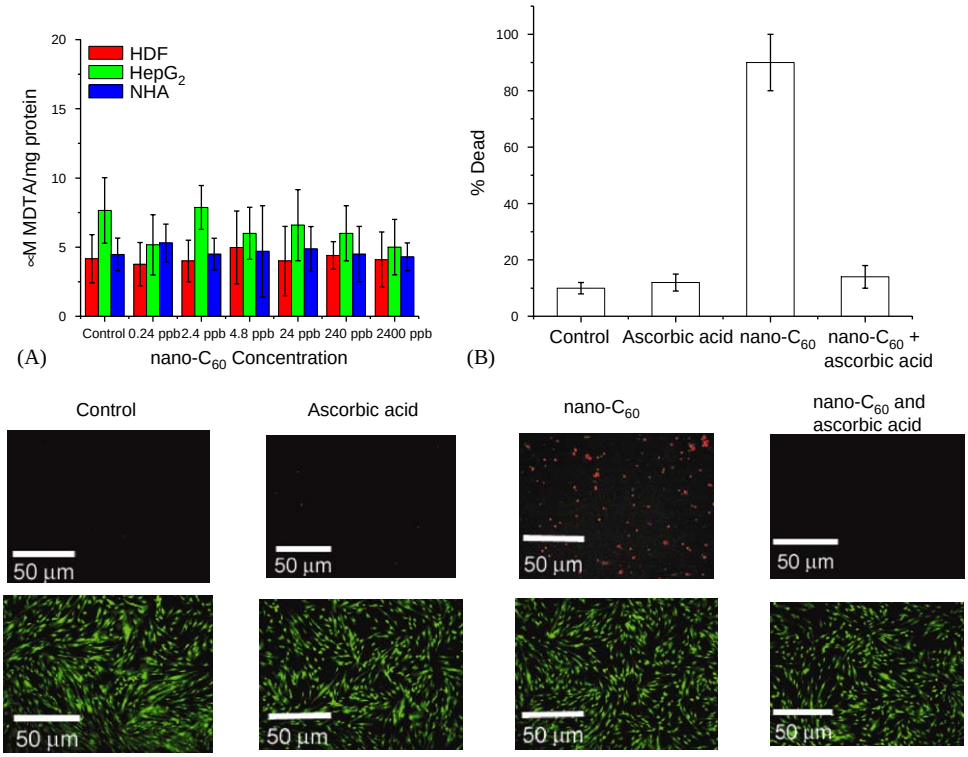

Fig. 5. Lipid peroxidation prevention and ascorbic acid toxicity. (A) MDTA does not increase at the 240 and 2400 ppb nano-C_{60} concentration when equal amounts of L-ascorbic acid is added to the cells. (B) Cell viability was determined in control cells, cells dosed with 240 ppb L-ascorbic acid, 240 ppb nano-C_{60}, and L-ascorbic acid/nano-C_{60}. (Bottom) Fluorescent micrographs of the viability of cells dosed with ascorbic acid, nano-C_{60}, and ascorbic acid/nano-C_{60}.

chemical properties, such as oxidant behavior in biological systems. Additionally, we note that many common antioxidants, including nitric oxide and vitamin E, will also act as prooxidants in certain biological environments [26,28–31,33].

Antioxidants, such as α-tocopherol, uric acid and L-ascorbic acid, typically prevent cellular damage that is caused by oxygen radicals [27,32]. With the addition of the antioxidant, L-ascorbic acid, the oxidative damage caused by ROS associated with the nano-C_{60} suspension was eliminated. In most of our experiments, the cell culture media itself contains antioxidants at relatively low concentrations. It may be that peroxidative processes begin at time zero, and that it takes more than 30 h to deplete the antioxidants in the cell culture media. In this interpretation, protection is extended beyond 48 h when L-ascorbic acid is added. Additional ascorbic acid is needed to protect the astrocytes, which are lipid rich cells. NHA were grown in media containing 1% ascorbic acid which protects these cells from oxidative stress generated during normal incubation. This initial concentration of L-ascorbic acid is substantially lower than the L-ascorbic acid added during the 48 h of nano-C_{60} exposure.

To date, there have no reports on long-term exposure to engineered nanomaterials, including fullerenes or fullerene derivatives. The only in vivo studies have focused on the short-term effects of nanomaterials instilled into the lungs of rodents. In that work carbon nanostructures, single-walled carbon nanotubes, were found to aggregate after exposure and apparently could clog small airways [21]. Additionally, short-term exposure of fullerenes with 2 or more covalently bonded water-solubilizing groups to cells in culture has also been reported [34–43].

C_{60} is alternately described in the literature as a nanomaterial and as a molecule. However, nano-C_{60}, a crystalline aggregate, is clearly an example of an engineered nanomaterial. Because of its size, a nanoparticle is potentially biologically active and could disrupt normal cellular processes; therefore, it is important to examine the potential biological effects of nanoparticles on the cellular level. This study, as well as our previous work, demonstrates that the biological behavior of nanoscale structures differs from both molecules and bulk materials, much in the same way that these materials exhibit unique chemical, physical and electronic properties [4].

5. Conclusion

The response of a cell to a nanomaterial can aid in the evaluation of the material for medical applications and

environmental fate. Given the enormous range of nanoparticle types, morphologies and surface chemistries, as well as the uncertain form of nanoparticles in future applications, toxicological testing that only provides a measure of hazard is not useful. Instead, toxicology in this emerging area must provide a basis for predicting systematically how a nanoparticle's biological behavior relates to its structure, composition and morphology. In vitro testing provides a cost-effective means for such studies, and as this report illustrates, cell culture experiments are well suited for developing mechanistic models to inform material development. We hope this work will set a standard for future efforts to characterize the environmental and health impacts of other classes of engineered nanoparticles. Ultimately, such proactive environmental and toxicological studies will be vital to ensure the nanomaterials design process yields both effective and safe technologies.

Acknowledgements

We thank Marcella Estrella for technical assistance with the cell cultures; Prof. Jane Grande-Allen for instrument use; and John D. Fortner, Delina Lyon, and Adina M. Boyd for supplying the nano-C_{60} sample. This work was financially supported by the Center for Biological and Environmental Nanotechnology (NSF EEC-0118007).

References

[1] Da Ros T, Prato M. Medicinal chemistry with fullerenes and fullerene derivatives. Chem Commun 1999;8:663–9.
[2] Da Ros T, Spalluto G, Boutorine A, Prato M. Fullerene derivatives as potential DNA photoprobes. Aust J Chem 2001;54:223–4.
[3] Colvin VL. The potential environmental impact of engineered nanomaterials. Nat Biotechnol 2003;21:1166–70.
[4] Sayes C, Fortner J, Lyon D, Boyd A, Ausman K, Tao Y, Sitharaman B, Wilson L, West J, Colvin VL. The differential cytotoxicity of water soluble fullerenes. Nano Lett 2004;4:1881.
[5] Andrievsky GV, Klochkov VK, Karyakina EL, McHedlov-Petrossyan NO. Studies of aqueous colloidal solutions of fullerene C-60 by electron microscopy. Chem Phys Lett 1999;300:392–6.
[6] Andrievsky GV, Klochkov VK, Bordyuh AB, Dovbeshko GI. Comparative analysis of two aqueous-colloidal solutions of C-60 fullerene with help of FTIR reflectance and UV-Vis spectroscopy. Chem Phys Lett 2002;364:8–17.
[7] Deguchi S, Alargova RG, Tsujii K. Stable dispersions of fullerenes, C-60 and C-70, in water. Preparation and characterization. Langmuir 2001;17:6013–7.
[8] Scrivens W, Tour J, Creek K, Pirisi L. Synthesis of 14C-labeled C60, its suspensions in water, and its uptake by human keratinocytes. J Am Chem Soc 1994;116:4517–8.
[9] Cheng XK, Kan AT, Tomson MB. Naphthalene adsorption and desorption from Aqueous C-60 fullerene. J Chem Eng Data 2004;49:675–83.
[10] Fortner J, Lyon D, Falkner J, Boyd A, Hotze E, Sayes C, Tao Y, Guo W, Ausman K, Colvin V, et al. C60 in water: nanocrystal formation and biological effects. Env Sci Technol 2005, in press.
[11] Legrand C. Lactate dehydrogenase (LDH) activity of the number of dead cells in the medium of cultured eukaryotic cells as marker. J Biotechnol 1992;25:231–43.
[12] Decker T, Lohmann-Matthes M-L. A quick and simple method for the quantitation of lactate dehydrogenase release in measurements of cellular cytotoxicity and tumor necrosis factor (TNF) activity. J Immunol Methods 1988;15:61–9.
[13] Mossman T. Rapid colorimetric assay for cellular growth and survival: application to proliferation and cytotoxicity assays. J Immunol Methods 1983;65:55–63.
[14] Stoscheck C. Quantitation of protein. Methods Enzymol 1990;182:50–69.
[15] Bradford M. A rapid and sensitive for the quantitation of microgram quantitites of protein utilizing the principle of protein-dye binding. Anal Biochem 1976;72:248–54.
[16] Aust S. CRC Handbook of methods for oxygen radical research. Boca Raton, Fl: CRC Press; c1985.
[17] Pap EHW, Drummen GPC, Winter VJ, Kooij TWA, Rijken P, Wirtz KWA, Op den Kamp JAF, Hage WJ, Post JA. Ratio-fluorescence microscopy of lipid oxidation in living cells using C11-BODIPY 581/591. FEBS Lett 1999;453:278–82.
[18] Drummen GPC, Op den Kamp JAF, Post JA. Validation of the peroxidative indicators, cis-parinaric acid and parinaroyl-phospholipids, in a model system and cultured cardiac myocytes. BBA-Mol Cell Biol Lipids 1999;1436:370–82.
[19] Derfus AM, Chan WCW, Bhatia SN. Probing the cytotoxicity of semiconductor quantum dots. Nano Lett 2004;4:11–8.
[20] Shvedova AA, Castranova V, Kisin ER, Schwegler-Berry D, Murray AR, Gandelsman VZ, Maynard A, Baron P. Exposure to carbon nanotube material: assessment of nanotube cytotoxicity using human keratinocyte cells. J Toxicol Env Health-Part A 2003;66:1909–26.
[21] Warheit DB, Laurence BR, Reed KL, Roach DH, Reynolds GAM, Webb TR. Comparative pulmonary toxicity assessment of single-wall carbon nanotubes in rats. Toxicol Sci 2004;77:117–25.
[22] Cusan C, Da Ros T, Spalluto G, Foley S, Janto J, Seta P, Larroque C, Tomasini M, Antonelli T, Ferraro L, et al. A new multi-charged C-60 derivative: synthesis and biological properties. Eur J Org Chem 2002;17:2928–34.
[23] Corona-Morales AA, Castell A, Escobar A, Drucker-Colin R, Zhang LM. Fullerene C-60 and ascorbic acid protect cultured chromaffin cells against levodopa toxicity. J Neurosci Res 2003;71:121–6.
[24] Dugan LL, Gabrielsen JK, Yu SP, Lin TS, Choi DW. Buckminsterfullerenol free radical scavengers reduce excitotoxic and apoptotic death of cultured cortical neurons. Neurobiol Dis 1996;3:129–35.
[25] Dugan LL, Turetsky DM, Du C, Lobner D, Wheeler M, Almli CR, Shen CK-F, Luh TY, Choi DW, Lin TS. Carboxyfullerenes as neuroprotective agents. Proc Natl Acad Sci USA 1997;94:9434–9.
[26] Bowry VW, Ingold KU, Stocker R. Vitamin-E in human low-density-lipoprotein—when and how this antioxidant becomes a prooxidant. Biochem J 1992;288:341–4.
[27] Burton GW, Ingold KU. Autoxidation of biological molecules. 1. The antioxidant activity of vitamin-E and related chain-breaking phenolic antioxidants invitro. J Am Chem Soc 1981;103:6472–7.
[28] Cillard J, Cillard P, Griffon B, Sinbandhit S, Sergent O. Nitric oxide as antioxidant and prooxidant in iron-mediated oxidative stress. Free Radical Biol Med 2004;36:S51.
[29] d'Eril GVM, De Luca G, Albertini R. An analogue of vitamin E has either antioxidant or prooxidant activity during oxidation of low-density lipoprotein: a descriptive and mechanistic study. Clin Chem 2001;47:A53.

[30] Hiramoto K, Ohkawa T, Oikawa N, Kikugawa K. Is nitric oxide (NO) an antioxidant or a prooxidant for lipid peroxidation? Chem Pharm Bull 2003;51:1046–50.
[31] Laskin JD, Heck DE, Gardner CR, Laskin DL. Prooxidant and antioxidant functions of nitric oxide in liver toxicity. Antioxid Redox Signal 2001;3:261–71.
[32] Packer JE, Slater TF, Willson RL. Direct observation of a free-radical interaction between vitamin-E and vitamin-C. Nature 1979;278:737–8.
[33] Ponthier JL, Joshi MS, Lancaster JR. Mechanisms of nitric oxide's antioxidant and prooxidant effects on oxidative killing of cells. Free Radical Biol Med 1999;27:S84.
[34] Tsao N, Luh TY, Chou CK, Chang TY, Wu JJ, Liu CC, Lei HY. In vitro action of carboxyfullerene. J Antimicrob Chemother 2002;49:641–9.
[35] Yang XL, Fan CH, Zhu HS. Photo-induced cytotoxicity of malonic acid C-60 fullerene derivatives and its mechanism. Toxicol Vitro 2002;16:41–6.
[36] Huang SS, Chen YH, Chiang LY, Tsai MC. Effects of hexasulfobutylated C-60 on the thalamic neurons in neonatal rat in vitro. Fullerene Sci Technol 1999;7:551–71.
[37] Sakai A, Yamakoshi Y, Miyata N. Visible light irradiation of 60 fullerene causes killing and initiation of transformation in BALB/3T3 cells. Fullerene Sci Technol 1999;7:743–56.
[38] Chen HCC, Huang YT, Pang VF, Liang SC, Chiang LY. Water-soluble C-60 and macrophages: morphologic features of FC4S-treated peritoneal macrophages in vitro and in vivo—a preliminary report. Fullerene Sci Technol 1999;7:505–17.
[39] Lin AMY, Chyi BY, Wang SD, Yu HH, Kanakamma PP, Luh TY, Chou CK, Ho LT. Carboxyfullerene prevents iron-induced oxidative stress in rat brain. J Neurochem 1999;72:1634–40.
[40] Zhang LM, Zhou LY, Martinez-Garcia M, Mendoza D, Drucker-Colin R. Effects of short-term and subchronical application of fullerene C-60 compound on guinea pig isolated myocyte electrical activity and rat chromaffin cell differentiation and proliferation. Fullerene Sci Technol 1998;6:815–25.
[41] Qian KX, Yan QF, Huang WD, Li WZ. Studies on the photoaction effect of C-60 on cancer cells in vitro and its mechanism. Prog Biochem Biophys 1997;24:237–41.
[42] Tsuchiya T, Oguri I, Yamakoshi YN, Miyata N. Novel harmful effects of 60 fullerene on mouse embryos in vitro and in vivo. FEBS Lett 1996;393:139–45.
[43] Yamago S, Tokuyama H, Nakamura E, Kikuchi K, Kananishi S, Sueki K, Nakahara H, Enomoto S, Ambe F. In-vivo biological behavior of a water-miscible fullerene—C-14 labeling, absorption, distribution, excretion and acute toxicity. Chem Biol 1995;2:385–9.